Ultra-stretchable and skin-mountable strain sensors using carbon nanotubes–Ecoflex nanocomposites

Morteza Amjadi[1]**, Yong Jin Yoon**[2] **and Inkyu Park**[1]

[1] Department of Mechanical Engineering and KI for the NanoCentury (KINC), Korea Advanced Institute of Science and Technology (KAIST), 291 Daehak-ro, Yuseong-gu, Daejeon 305-701, Korea
[2] School of Mechanical & Aerospace Engineering, Nanyang Technological University (NTU), 50 Nanyang Ave, 639798, Singapore

E-mail: inkyu@kaist.ac.kr

CrossMark

Abstract

Super-stretchable, skin-mountable, and ultra-soft strain sensors are presented by using carbon nanotube percolation network–silicone rubber nanocomposite thin films. The applicability of the strain sensors as epidermal electronic systems, in which mechanical compliance like human skin and high stretchability ($\varepsilon > 100\%$) are required, has been explored. The sensitivity of the strain sensors can be tuned by the number density of the carbon nanotube percolation network. The strain sensors show excellent hysteresis performance at different strain levels and rates with high linearity and small drift. We found that the carbon nanotube–silicone rubber based strain sensors possess super-stretchability and high reliability for strains as large as 500%. The nanocomposite thin films exhibit high robustness and excellent resistance–strain dependency for over ∼1380% mechanical strain. Finally, we performed skin motion detection by mounting the strain sensors on different parts of the body. The maximum induced strain by the bending of the finger, wrist, and elbow was measured to be ∼ 42%, 45% and 63%, respectively.

S Online supplementary data available from stacks.iop.org/NANO/26/375501/mmedia

(Some figures may appear in colour only in the online journal)

1. Introduction

Strain sensors transduce mechanical deformations to electrical signals such as a change of the capacitance or resistance. Even though commercially available strain sensors based on metal foils and semiconductors have a well-established technology and low cost of fabrication, they possess very poor stretchability ($\varepsilon < 5\%$) due to the brittleness of the sensing materials [1–4]. On the other hand, interest is dramatically arising in stretchable, skin-mountable, and wearable electronic devices due to their facile interaction with the human body and long-term monitoring capabilities under large strain conditions. Examples of such electronic devices include stretchable, skin-mountable, and wearable strain sensors for human motion detection [1, 2, 4−7], flexible electronic skins for pressure visualization [8, 9], or skin-mountable devices for human body temperature monitoring [10]. Among those innovative electronic devices, highly stretchable ($\varepsilon > 100\%$), skin-mountable, and wearable strain sensors (also known as 'epidermal' electronic devices) are needed because of their potential applications such as rehabilitation/personalized health monitoring [11–13], sport performance monitoring [14, 15], robotics [2, 16], and entertainment technology (e.g. motion capture for games and animations) [1, 17]. As alternatives to conventional strain gauges, capacitive and resistive types of stretchable strain sensors have been developed by using nanomaterials and micro/nanostructures [1, 3–5, 18]. In particular, percolation

networks of nanomaterial/polymer composites can maintain their electromechanical stability for high strains. High performance stretchable capacitive type strain sensors were fabricated by laminating a flexible dielectric layer between a pair of stretchable electrodes mainly made of carbon nanotubes (CNTs) and Ag nanowires (AgNWs) [16, 18–23]. Super-stretchable ($\varepsilon \sim 300\%$) strain sensors with excellent linearity, hysteresis, and creep performance were reported using Dragon Skin® as a dielectric layer and CNT thin films as stretchable electrodes [18]. However, very low sensitivities or gauge factors (GFs $\leqslant 1$), unpredictable response due to unstable overlaps of the capacitive area, and capacitive interaction with the human body are among the main drawbacks of capacitive type strain sensors, limiting their applications as epidermal devices [18, 21]. In parallel, resistive type flexible strain sensors have been achieved using composites of flexible substrates and nanomaterials such as carbon nanotubes (CNTs) [5, 24, 25], nanowires (NWs) [1, 26, 27], nanoparticles (NPs) [28] and graphene [2, 3, 6, 25, 29, 30]. The resistance–strain dependency in these types of strain sensor originates from geometrical changes [3, 4], change of the bandgap interatomic spacing [4, 31], crack propagation in the sensing thin films [5, 29, 31], disconnection between sensing elements [1, 3, 4, 26, 32], and tunneling effect [25, 31, 33, 34]. Despite the stretchability of the resistive type strain sensors, they typically respond to applied strains with low GFs, high nonlinearity, and hysteresis [2, 4, 5, 21, 24, 29, 32, 35, 36]. For instance, strain sensors made of aligned CNT thin films on flexible substrates show excellent stretchability ($\varepsilon \sim 280\%$) with high reliability. However, these sensors suffer from very low sensitivities (GFs $\leqslant 0.82$) and high hysteresis [5].

CNTs have been widely used in flexible electronic devices [37, 38], sensors and actuators [5, 39], and biomaterials [40–42] due to their excellent mechanical, electrical, and thermal properties [43]. A percolation network of CNTs coupled with elastomeric polymers is able to maintain electrical conductivity even under high stretching due to the continual contact between CNTs within the percolation network. On the other hand, polydimethylsiloxane (PDMS) has commonly been utilized as a flexible substrate integrated with nanomaterials for strain sensing due to its transparency, curability, non-toxicity, and biocompatibility [44, 45]. Numerous types of strain sensor have been explored by the use of CNTs as fillers and PDMS as flexible substrates. However, most of the previously fabricated strain sensors exhibit highly nonlinear responses and high hysteresis with lower stretchability required for epidermal electronic applications [5, 24, 25, 46]. Hysteresis is mainly caused by the friction and poor interfacial adhesion between CNTs and the polymer matrix [1, 24]. In addition to the poor sensing performance of the CNT–PDMS composite based strain sensors, PDMS substrates bear much higher Young's modulus (0.4–3.5 MPa) than that of human skin (25–220 kPa), and this discrepancy becomes larger when PDMS is mixed with CNTs [1, 4, 16, 47–49]. Also, stiffening and aging of PDMS due to water absorption is another special restriction of the use of PDMS as a substrate for skin-mountable electronic devices

[50]. Aging of PDMS can make it stiffer and more brittle. Therefore, delamination and sliding of strain sensors occur when they are mounted on the human skin, restricting their applications as epidermal devices. As an example, we have developed stretchable and sensitive strain sensors based on AgNW network–PDMS nanocomposites for human motion detection [1]. However, sliding of the strain sensors on the human body or clothing was observed during experiments. Sliding of the strain sensors increases noise and inaccuracy in the response and underestimates the actual strains occurring on the human skin. Hence, high performance strain sensors made of softer materials than PDMS are required for accurate detection of the human skin motion. Such devices could be directly laminated onto the complex and curvilinear surface of the human body without any mechanical constraints, slippage, or delamination.

Herein, we report highly flexible, super-stretchable, and ultra-soft strain sensors based on nanocomposites of the CNT percolation networks–silicone rubber (Ecoflex®, platinum-catalyzed silicone). We selected Ecoflex as our flexible substrate for several reasons. First, we found that ultra-soft Ecoflex with a Young's modulus of $\sim$125 kPa exhibits mechanical compliance as high as that of the human skin and approaches the requirements for the human epidermis [4, 51]. Secondly, we believe that strain sensors made of the CNT–Ecoflex nanocomposite will possess high performance characteristics due to strong interfacial bonding between the CNTs and the Ecoflex matrix. Thirdly, as compared to the aging effect of PDMS, Ecoflex is an environmentally stable polymer due to its water resistivity and is suitable for long-term sensing applications. Lastly, biocompatible Ecoflex could be easily utilized as a skin-mountable device without any restriction, skin irritation, or discomfort. The performances of the strain sensors including stretchability, linearity, hysteresis, drift, long-term stability, and response time were shown to be excellent as compared with previously developed stretchable strain sensors [2, 4, 5, 24]. The CNT–Ecoflex nanocomposite based strain sensors possess super-stretchability of $\sim 500\%$, high linearity ($R^2 > 0.95$), very high reliability, and fast response speed with small hysteresis and drift, simultaneously. The strain sensors are independent of strain rate and their sensitivity can be tuned by the number density of the CNT networks. To illustrate the applicability of our strain sensors as epidermal devices, we conducted human skin motion detection by mounting the strain sensors on the human skin. The strain sensors respond to human skin motion with good sensitivity, fast response, and high repeatability.

2. Experimental section

2.1. Preparation of the CNT solution

Multi-walled carbon nanotubes (MWCNTs) with an average length of 5–20 μm and average diameter of 16 $\pm$ 3.6 nm were purchased from Hyosung Co., South Korea. 0.05%wt. of non-functionalized CNTs in isopropyl alcohol (IPA) was sonicated for an hour and the solution was further stirred for
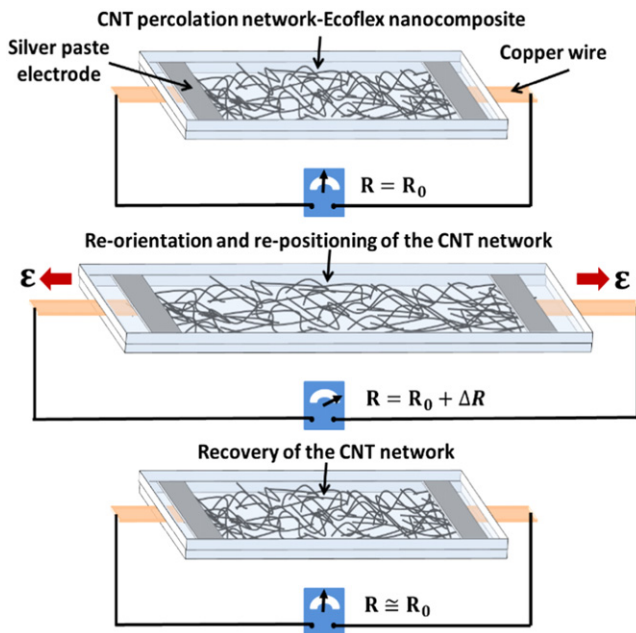
Scheme 1. Structure and basic working principles of the CNT–Ecoflex nanocomposite strain sensors. The percolation network of the CNTs experiences re-orientation and re-positioning of CNTs by the external tensile strain. When the strain is released, the elastic force of Ecoflex results in the recovery of the original percolation network and complete recovery of the electrical resistance.

another hour to release the agglomerated CNTs and perfectly suspend all CNTs in the IPA medium. The uniform suspension of CNTs in IPA was stored for further experiments.

2.2. Fabrication of samples

Scheme 1 illustrates the structure and basic principles of our strain sensors. The strain sensors consist of CNT–Ecoflex nanocomposite thin films laminated between the top and bottom layers of Ecoflex. When the strain sensors are stretched out, re-orientation and re-positioning of CNTs within the percolation network increases the base resistance of the strain sensors. Moreover, upon relaxation of the strain sensors, re-establishment of the percolation network inspired by the elastic force of Ecoflex recovers the resistance. The fabrication processes of the CNT–Ecoflex nanocomposite thin films is schematically illustrated in figure 1(a). Here, instead of very complex and difficult dispersion methods (i.e. dispersion of CNTs inside the polymer matrix) for the fabrication of nanocomposites [52], we successfully fabricated the CNT–Ecoflex nanocomposite by the infiltration of the liquid polymer inside the porous CNT network thin film in a controllable manner [1, 20, 53]. Air-spray coating was utilized as a facile, scalable, and low cost method for the deposition of the CNT thin films (spray pressure @ 2 bars). The CNT solution was coated on the patterned polyimide (PI) films patterned with a plotter (GRAPHTEC, CE2000-120) at 100 °C to obtain the CNT percolation thin films. Both the resistance and thickness of the CNT thin films could be controlled by the amount and density of the sprayed solution. The CNT thin films were annealed at 200 °C for 30 min to remove residual organic

components. In order to avoid the soaking of the liquid elastomeric polymer inside the space of the connected CNTs, which dramatically decreases the electrical conductivity of the percolation network, the annealed CNT thin films were further pressed by a PI stamp for better connection between adjacent CNTs. Then, the CNT thin films were transferred to the polymer medium by casting the liquid Ecoflex (with an average thickness of 0.5 mm) on top of the patterned CNT thin films and curing it at 70 °C for 2 h. Afterwards, the Ecoflex layer embedded with the CNT film was peeled off from the PI substrate. All CNTs were buried just below the surface of Ecoflex due to the penetration of the liquid Ecoflex into the network of the CNT thin film to form a robust nanocomposite of CNTs and Ecoflex. Then, copper wires were connected to the two ends of the CNT thin film with silver paste. Finally, another layer of liquid Ecoflex with the same thickness ($\sim$ 0.5 mm) was cured on top of the CNT thin film to form a sandwiched structure (i.e. Ecoflex layer/CNT thin film nanocomposite/Ecoflex layer).

2.3. Rosette type strain sensors

Rosette type strain sensors were fabricated first by patterning the PI film using a plotter (see 'Fabrication of the rosette type strain sensors' section in the supplementary information for more detail). Then, a high density CNT thin film was spray coated in the electrode areas. Next, a very low density CNT thin film was coated in the sensing area, and the whole deposited CNT thin film was transferred onto the Ecoflex matrix. Finally, the peeled-off CNT thin film was covered with another layer of Ecoflex.

3. Results and discussion

Figure 1(b) illustrates the transferred CNT thin films on the polymer matrix with different shapes, good stretchability, softness, and robustness. Strain sensors were fabricated by transferring the slender rectangular patterned CNT thin films (3 mm $\times$ 45 mm) onto the Ecoflex matrix. Figure 1(c) shows photographs of the fabricated strain sensors under bending and twisting with ultra-softness and flexibility. They can be directly mounted on the human skin with perfect contact and negligible slippage. Figure 1(d) illustrates photographs of a strain sensor at its original length and with over 500% strain, showing the super-stretchability of the strain sensor.

Figure S2(a) in the supplementary information illustrates a transmission electron microscopy (TEM) image of the surface of the CNT thin film transferred onto the polymer substrate. CNTs are randomly and uniformly dispersed on the surface of the Ecoflex layer without voids and detachment, showing successful transfer of the CNT thin film from the PI substrate onto the Ecoflex film. When the liquid Ecoflex is cast onto the CNT network, it penetrates into the porous network of the CNTs due to the low viscosity of the liquid Ecoflex and forms a robust nanocomposite of CNTs and Ecoflex. It should be noted that the selection of the donor substrate is very important for the successful transfer of the
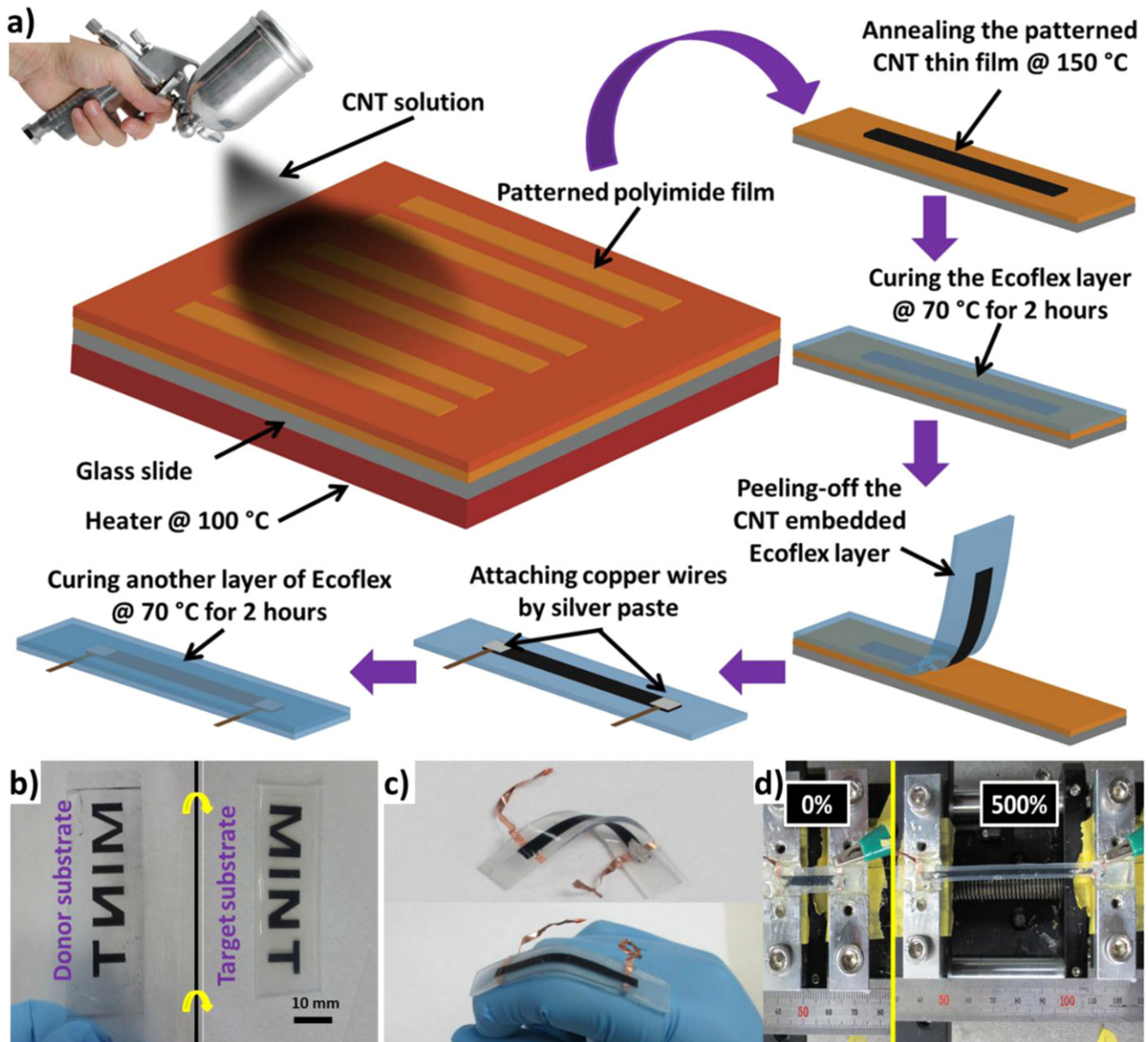
Figure 1. Fabrication of the CNT–Ecoflex nanocomposite-based strain sensor: (a) fabrication process of the sandwich type CNT–Ecoflex nanocomposite-based strain sensors. (b) Photograph of the transferred CNT thin films with different pattern shapes from donor substrate to the Ecoflex (target) substrate. (c) Photographs of the fabricated sandwich structured strain sensor when it is bent and twisted. (d) Photograph of a strain sensor at the initial length and with 500% stretching.

thin film to the target substrate. We used PI film as the donor substrate due to its very low surface energy ($\sim 44\,\mathrm{mJ\,m^{-2}}$) and high contact angle ($\sim 74°$), ensuring weak adhesion with the coated CNT thin films [54]. Therefore, the CNT thin films can be easily detached from the PI substrate. For example, Ecoflex film did not completely peel off from the glass substrate because of the strong binding of the CNT thin films and Ecoflex with glass (see figure S3 in the supplementary information). Figure S2(b) shows a high resolution TEM image of a single CNT embedded on the surface of the Ecoflex layer. As the figure depicts, the whole structure of the CNT is covered by Ecoflex molecules, providing strong adhesion between the CNTs and Ecoflex. It is noteworthy to

mention that we proposed the sandwiched structure to reduce the wrinkling and plastic deformation of the CNT–Ecoflex nanocomposite layer, which occur in the case of the simple embedded structure (i.e. a nanocomposite thin film on top of the Ecoflex layer without an additional Ecoflex cover layer), inducing high nonlinearity and unstable electromechanical behavior (see figure S4 in the supplementary information) [1, 25, 45]. In a bilayer system such as the simple embedded sample with the stiff CNT–Ecoflex nanocomposite layer on the compliant Ecoflex substrate, spontaneous wrinkle patterns emerge to release the compressive strain caused by mechanical instability [1]. In contrast, the sandwich structure sensor prevents the wrinkling by forming a symmetric layer structure
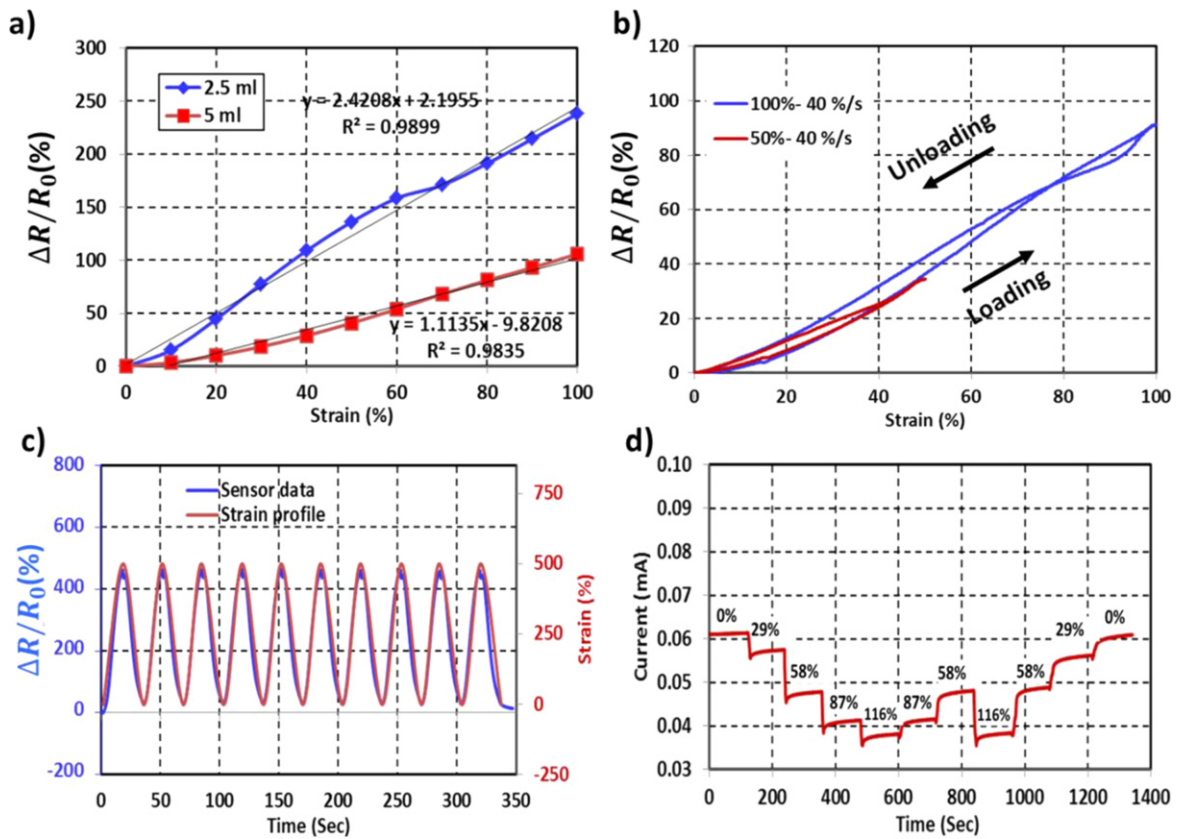
Figure 2. Electromechanical characterization of the CNT–Ecoflex nanocomposite based strain sensor: (a) piezoresistive response of two strain sensors with different network densities. (b) Hysteresis performance of a strain sensor at different strain levels. (c) Response of a strain sensors to 10 cycles of loading/unloading from $\varepsilon = 0\%$ to $\varepsilon = 500\%$. (d) Drift performance of a strain sensor with several random strains.

and strengthening the CNT–Ecoflex nanocomposite layer. In addition, the sandwich structure protects the nanocomposite thin film from physical contact and damage by the complete coverage of the thin film on both sides.

In order to characterize the electromechanical behavior of the CNT–Ecoflex nanocomposites, they were clamped to a motorized moving controller (Future Science Motion Controller, FS100801A1P1). Then, strain/release cycles with different strain levels and rates were applied to the strain sensors while the current changes were measured under a constant voltage of 4 V with a potentiometer (CH Instruments, Electrochemical Workstation, CHI901D). In some strain sensors, the initial resistance was increased by ∼10% in the first few stretching/releasing cycles, while the response was highly reproducible afterwards. This could be due to the permanent replacement of some CNTs within the Ecoflex matrix in the first cycle. Figure 2(a) shows a typical curve of the relative change in resistance against the applied strain for strain sensors with different CNT network densities. The density of the CNT network was controlled by the amount of spray-coated CNT solution. For example, strain sensors with initial resistances of 15.5 and 134 kΩ were achieved when 5 and 2.5 ml of the CNT solution were coated on the patterned PI film ($15 \times 80\,\mathrm{mm}^2$). As the figure depicts, the strain sensors respond to the applied strain with excellent linearity ($R^2 > 0.98$) for a wide range of strains (from 0% to 100%). The GF, the slope of the relative change of resistance with

respect to the applied strain, increases by lowering the network density in a controllable manner. We observed this correspondence during all of the experiments. The change of the electrical conductance within the percolation network is the main reason for the resistance–strain dependency of the nanocomposite. Upon stretching, CNTs are separated apart within the percolation network, increasing the tunneling resistance between adjacent CNTs and consequently reducing the electrical conductance [4, 24]. The sensitivity is much higher in the low density network since fewer parallel conduction pathways contribute to the electrical conductivity. We believe that much higher sensitivity can be achieved by the precise control of the deposition parameters. Figure 2(b) presents the hysteresis performance of a strain sensor (5 ml CNT solution coating) at strains of $\varepsilon = 50\%$ and 100% with a strain rate of 40% s^{-1}. As the figure illustrates, the electrical resistance of the strain sensor was fully recovered after releasing it from the strain with negligible hysteresis. In addition, we found that the performances of the strain sensors are almost independent of the strain rates, see figure S5 in the supplementary information. Figure 2(c) shows the dynamic response of a strain sensor under repeated stretching/releasing cycles with 0–500% tensile strain. The resistance of the sensor was almost recovered after releasing it from 500% tensile strain, indicating the super-stretchability of our strain sensors. As illustrated in the figure, there are excellent overlaps between the loading profile and the response of the
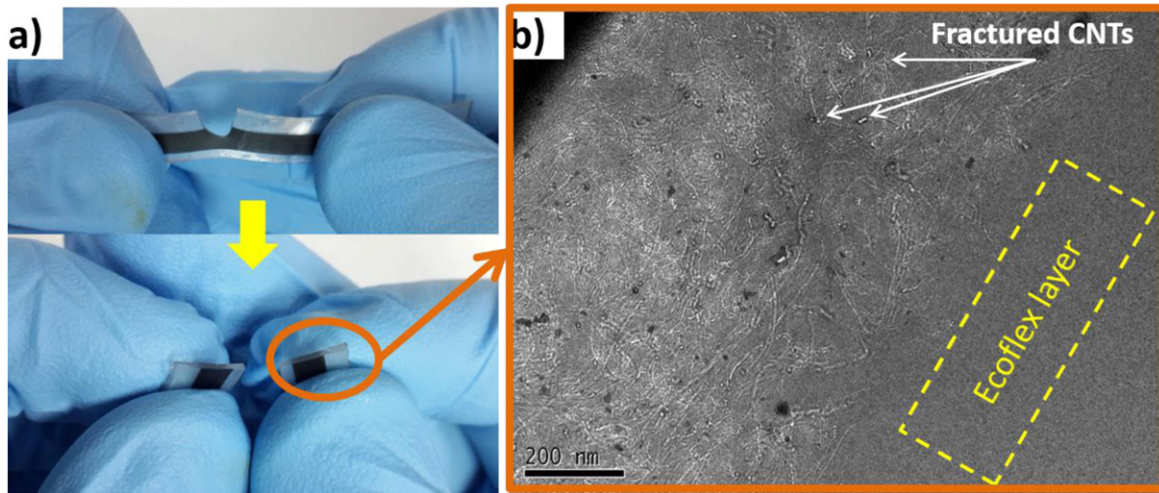
Figure 3. TEM observation of a cross-section of the CNT–Ecoflex based nanocomposite: (a) ripping of the CNT–Ecoflex nanocomposite film under tensile loading. (b) Cross-sectional image of the nanocomposite layer in the cracked zone.

sensor with excellent linearity and hysteresis performance. We also examined the drift and overshoot behavior of our strain sensors. As shown in figure 2(d), the strain sensor was subjected to random strains and held at each strain for 120 s, while the current was measured. The strain sensor exhibits a small overshoot by the strain change, which may be due to the stress relaxation and viscoelastic nature of the polymers [32, 55]. When the elastomer is stretched by external tensile loading, tensile stress develops in the elastomer and is then transferred to the CNT–elastomer nanocomposite. This causes re-arrangement and re-orientation of the CNTs and the electrical resistance of the CNT network is increased as a consequence. However, the tensile stress is reduced by the stress relaxation effect and therefore, the positions and orientations of the CNTs are partially restored as time passes. Therefore, the electrical resistance is gradually decreased when a constant tensile strain is applied for a longer duration. After a 120 s holding time, the overshoot resistance value was decreased by 3.4, 5.2, 6.3, and 6.8% at strain values of 29%, 58%, 87%, 116%, respectively. It can be clearly seen that the steady state current value remains almost identical under the same strain (e.g. at 58% of strain, the steady state current was 47.8 μA with a small standard deviation of 0.8 μA) (see figure S6 in the supplementary information). Next, to evaluate the failure strain of the sensor, it was subjected to a continuously increasing strain with a rate of 30% s^{-1}, as shown in figure S7. The film was electromechanically robust for over ~1380% stretching and responded to the applied strain with good sensitivity and linearity, although we could not measure the failure strain level due to the limitations of our experimental setup. The very high failure strength of the nanocomposite may be due to the excellent interfacial bonding and load transfer between the CNT fillers and the Ecoflex matrix. Due to the strong bonding between the CNTs and Ecoflex, no slipping or detachment between them can occur. When a high strain is applied, the complicated and entangled CNT network is stretched and unfolded but no breakage or fracture occurs due to the strong bonding between the CNTs and Ecoflex.

Therefore, very high strain can be applied to the CNT–Ecoflex composite strain sensor without causing electrical failure. The performance of the CNT–Ecoflex nanocomposite based strain sensors, especially in terms of linearity, hysteresis, and stretchability are much better than previously reported strain sensors made of carbon-based nanomaterials/polymer composites [2, 4–7, 24, 32] with nonlinear response and hysteresis, ZnONWs/polymer composites with linear response and stretchability of up to 50% [27], and AgNWs/polymer nanocomposites with linear response of up to 40% and stretchability of 70% [1, 26]. A comparison between the performances of some newly developed strain sensors and our strain sensors is provided in table S1 in the supplementary information.

We believe that the linearity, hysteresis performance, and durability of the nanocomposite based strain sensors are mostly affected by the structure of the strain sensors (i.e. removing the plastic deformation/wrinkling of the nanocomposite thin film by the sandwiched structure), the properties of the polymer, and the interaction between the fillers and the polymer matrix [5, 25]. Furthermore, hysteresis is mainly caused by the friction force between the filler elements and the matrix due to the slippage of fillers under stretching and the delay time associated with the re-establishment of the percolation network upon release [45, 56]. To address this, we examined the interfacial adhesion between the CNTs and the Ecoflex matrix through TEM observations in pre-cracked walls. A small crack was induced in a nanocomposite thin film and then the nanocomposite film was ripped into two parts by tensile loading (i.e. the crack was in the transverse direction of stretching), as shown in figure 3(a). The cross-sections of the cracked zones were observed by TEM imaging to examine the interactions between the CNTs and Ecoflex. Figure 3(b) indicates the cross-sectional view of the CNT–Ecoflex nanocomposite layer where the sample was ripped. Even though there are a few CNTs peeled off the Ecoflex matrix (dark holes), most of the cross-linked CNTs are fractured in the crack zone, showing the strong binding between
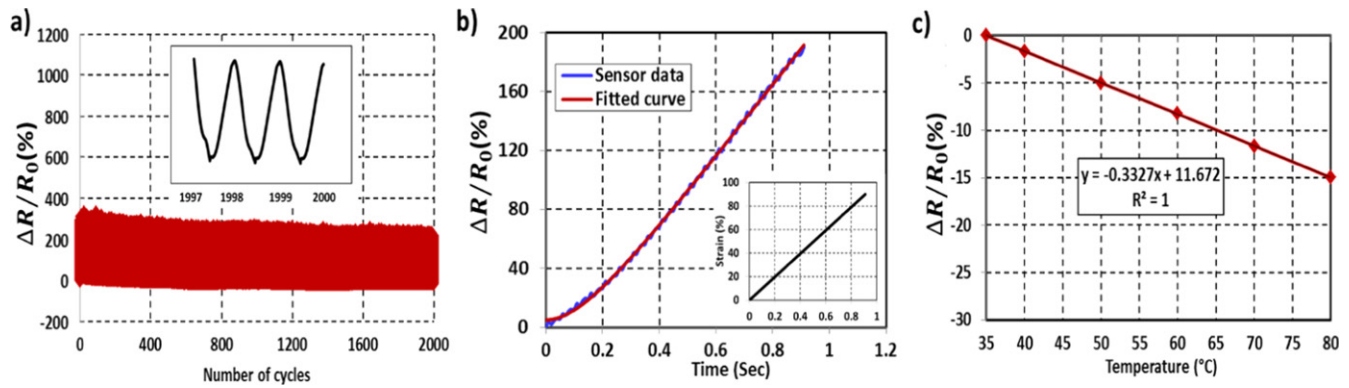
Figure 4. Additional electromechanical characterization of the CNT–Ecoflex based nanocomposite stratin sensor: (a) long-term stability of a strain sensor over more than 2000 cycles ($\varepsilon = 0\%$ to $\varepsilon = 300\%$). (b) Response of a strain sensor to a ramp strain profile; inset, strain profile. (c) Relative change of the resistance versus temperature for a strain sensor.

the CNTs and the Ecoflex matrix. Moreover, the strong binding between the CNTs and Ecoflex could be due to the mechanical interlocking of the CNTs and polymer molecules owing to the very low viscosity of the liquid Ecoflex, covalent chemical bonding and non-covalent bonding like van der Waals and electrostatic forces [36, 45, 57]. Previous studies indicate that the interfacial binding mechanism between CNTs and polymers is still controversial. For example, in certain polymers, strong binding between CNTs and polymers was observed, although there are several contrasting findings [36, 57, 58]. In our case, the excellent hysteresis performance of the CNT–Ecoflex nanocomposite based strain sensors is achieved by strong binding between the CNTs and the Ecoflex matrix. Moreover, CNTs have excellent elastic properties with tensile strength of up to 40% [59], enabling the CNTs to move and stretch with the elongation of Ecoflex. The CNT–Ecoflex nanocomposite consists of numerous CNTs that are entangled and folded in a complex network. Therefore, when an external strain is applied, unfolding of the entangled CNTs is more probable than stretching in their axial directions. Also, slippage of the CNTs inside the Ecoflex matrix is less probable owing to the excellent elastic behavior of the CNTs as well as the strong binding between the CNTs and Ecoflex, minimizing the hysteresis effect. Interestingly, an increase of the initial resistance in the first cycle under high strain level (>100%) can also be identified with this model. High strains cause some CNTs to exceed their elastic elongation limit, thus leading to permanent sliding of these CNTs from the Ecoflex matrix or fracturing of some CNTs, raising the initial resistance [60]. Being different from conventional metal foil based strain sensors, the resistance–strain dependency of the CNT–Ecoflex nanocomposite strain sensors is not mainly due to the geometrical changes in the sensing area. Instead, a significant contribution originates from the tunneling effect between the CNTs and structural deformation of the CNTs themselves [24, 36]. Electrons can tunnel through the polymer matrix when the distance between two neighboring CNTs is within a cut-off distance. The tunneling resistance is highly dependent on the distance between the CNTs. Moreover, stretching of the nanocomposite thin film results in the increase of the interspace at the CNT–CNT junctions and consequently an

increase of the tunneling resistance [24]. We believe that besides the deposition parameters, the sensitivity of the strain sensors can be improved by using short length CNTs. With the same density, a larger number of tunneling junctions exist for a short length CNT network, enhancing the piezo-resistivity. However, this may also compromise the linearity and stretchability of the strain sensor. In our previous work, we identified that the main mechanism for the piezoresistivity of the AgNWs/PDMS nanocomposite is the disconnection between the AgNW–AgNW junctions caused by sliding and complete recovery of AgNWs within the PDMS matrix due to the rigidity of NWs with small fracture strains of 0.92–1.64% and weak interfacial adhesion between the AgNWs and PDMS [1, 20]. However, the dominant reason for the piezoresistivity of the CNT–Ecoflex nanocomposites is the tunneling effect due to the elastic behavior of CNTs and strong interfacial binding between the CNTs and Ecoflex, rather than disconnection between neighboring CNTs [36, 61].

Further tests were carried out to evaluate the long-term stability, response time, and temperature dependency of the strain sensors. A strain sensor was subjected to more than 2000 cycles of repeated loading/unloading (from $\varepsilon = 0\%$ to $\varepsilon = 300\%$) with a strain rate of 20% s^{-1}. Figure 4(a) shows the long-term performance of the strain sensor with excellent stability and recoverability. We could observe a small drift in the resistance at the loading state due to the possible sliding of the strain sensor from the clamps at such a high level of strain. However, the base resistance of the strain sensor was almost constant under cyclic loading, showing the excellent reliability of the strain sensors. To the best of our knowledge, this is the only reported strain sensor with this level of stretchability and reliability to date. For example, a stretchability up to $\sim 200\%$ with complete recovery of the resistance after 3300 cycles in the case of CNTs/PDMS composites and a stretchability up to $\sim 200\%$ with complete recovery of capacitance after 1800 cycles for CNTs/Dragon rubber composite based strain sensors have been reported in the literature [5, 18]. The high stretchability of our strain sensors is due to the ultra-high stretchability of Ecoflex itself and the strong binding between the CNTs and Ecoflex.
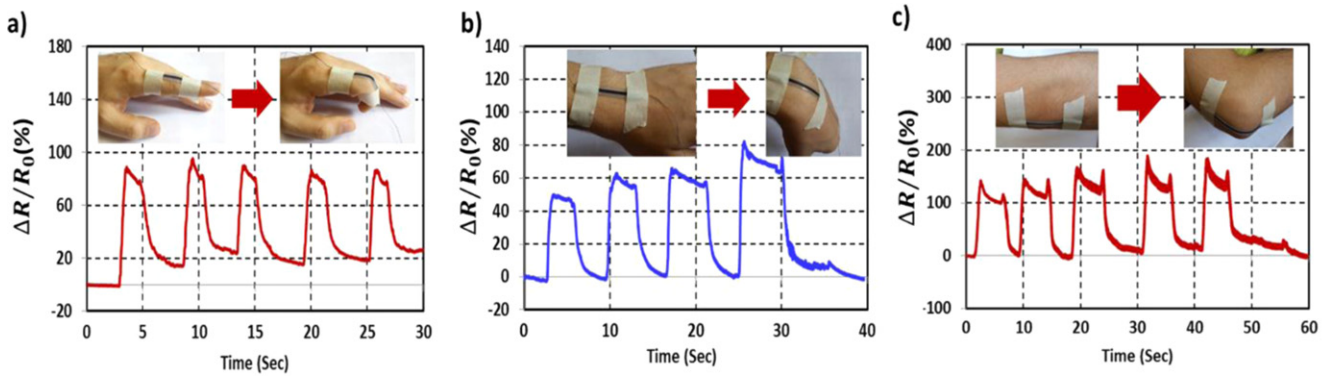
Figure 5. Application of the CNT–Ecoflex nanocomposite based strain sensors to human motion detection: (a) finger joint motion detection by using CNT–Ecoflex nanocomposite based strain sensors; inset, photograph of the mounted strain sensor. (b) Wrist joint detection by attaching the strain sensor on the joint of the wrist; inset, photograph of the mounted strain sensor. (c) Elbow joint motion detection; inset, a strain sensor mounted on the elbow joint.

To calculate the response time of the strain sensors, a strain sensor was linearly stretched from 0% to 90% with a high strain rate of 100% s^{-1} (i.e. ramp strain profile, the inset of figure 4(b)) while the response of the strain sensor was measured. We found that the response of the sensor could be assumed to be a first order dynamic system, as shown in figure 4(b). The response of a first order system is given by:

$$\frac{C(S)}{R(S)} = \frac{1}{\tau S + 1}$$

where τ is the time constant of the system, and $C(S)$ and $R(S)$ are the Laplace functions for output and input, respectively. For a ramp input, the Laplace functions of the load and response are $R(S) = k/S^2$ and $C(S) = k/(S^2(\tau S + 1))$, respectively. Thus, the inverse Laplace transformation of the output response is:

$$C(t) = k\left(t - \tau\left(1 - e^{\left(-\frac{t}{\tau}\right)}\right)\right)$$

Our experimental data was fitted by the above equation and the calculated k and τ values are 2.44 and 0.144 s, respectively. Therefore, the 90% time constant ($\tau_{90\%}$) for our strain sensors is ∼332 ms. If we consider the unknown delay of the measurement system, the actual time constant for the sensor itself would be even shorter than this. The response time of the CNT–Ecoflex nanocomposite strain sensors is slightly larger than that of our AgNWs–PDMS nanocomposite strain sensors (∼200 ms) [1]. This could be due to the softness of the Ecoflex matrix, providing a lower recovery force for the fast re-establishment of the CNT percolation network.

By nature, the conductivity of all metal or semi-conductor materials is affected by the temperature. However, linear resistance–temperature dependency is desirable for sensors since the temperature effect can be compensated for by offset calibration and Wheatstone bridge configuration or more precisely with thermometers [4, 5]. A strain sensor was put into a convection oven while its temperature was gradually increased from 35 °C to 80 °C. Figure 4(c) shows the

relative change in resistance for the sensor with the applied temperature. The CNT–Ecoflex nanocomposite shows a negative temperature coefficient with excellent linearity ($R^2 = 1$) and with a slope of $(\Delta R/R_0)/\Delta T = 0.33\%$ K^{-1}. This linear temperature response of our sensor is superior to the nonlinear temperature dependency of nanocomposites made of MWCNTs and PDMS, styrene-(ethylene-co-butylene)-b-styrene (SEBS), epoxy and polypropylene (PP) [46, 62–64].

As our experimental results reveal, the CNT–Ecoflex nanocomposite based strain sensors are super-stretchable, ultra-soft, and high performance strain sensors. The strain sensors could be utilized as epidermal electronic systems in which the strain sensors could be easily mounted on the human skin without any discomfort. To show the applicability of our strain sensors as skin-mountable electronic devices, they were attached to different parts of the body for skin motion detection. For example, we conducted index finger, wrist, and elbow joint motion detection using a CNT–Ecoflex nanocomposite based strain sensor with GF ∼ 1.75. The strain sensor was directly mounted to the skin of the finger by using an adhesive bandage attached to the electrode parts of the strain sensor, see inset of figure 5(a). The strain sensor has perfect adhesion to the skin without any sliding or delamination. The response of the strain sensor to bending/relaxing with excellent sensitivity is illustrated in figure 5(a). The more bending the sensor undergoes, the greater the increase in the resistance. The maximum measured strain upon bending of the index finger is ∼ 42%, in good agreement with previously reported strains (35%–45%) [2, 7, 21]. Wrist bending detection was conducted by attaching the strain sensor to the wrist joint, as shown in the inset of figure 5(b). The response of the strain sensor was measured upon downward bending and recovery to a straight position of the wrist. As figure 5(b) depicts, the strain sensor responds to cyclic bending/relaxing in a reversible manner (see 'wrist motion detection video' in the supplementary information). The maximum strain for the wrist bending is measured as about ∼ 45%. We also conducted elbow joint bending measurements as shown in the inset of figure 5(c). The maximum strain value measured by
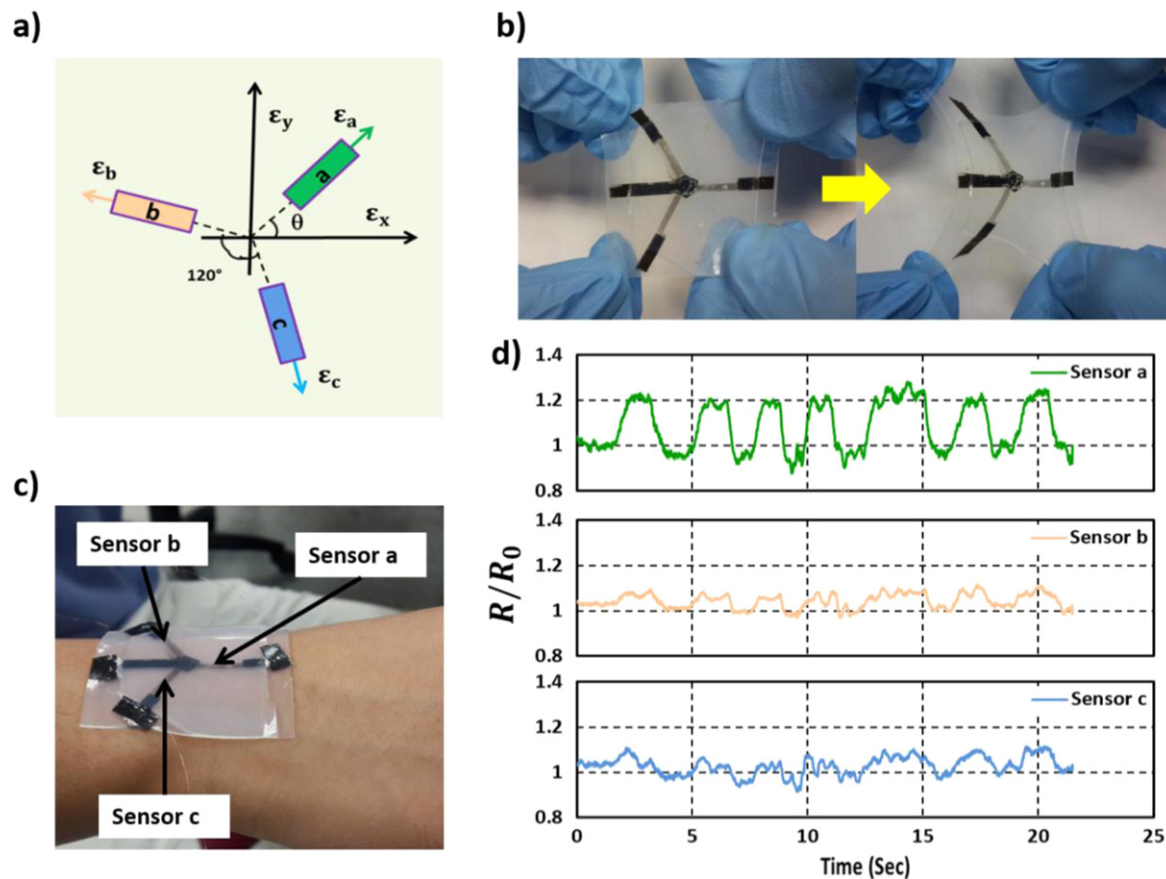
Figure 6. Multi-axial skin strain measurement by using a rosette type CNT–Ecoflex nanocomposite based strain sensor: (a) configuration of the rosette type strain sensor. (b) A rosette type strain sensor in its original state and when biaxially stretched. (c) Photograph of the rosette strain sensor attached to the wrist joint. (d) Normalized change of the resistance for the rosette strain sensor composed of sensor a, b, and c upon bending/relaxing of the human wrist.

the bending of the elbow is about $\sim 63\%$. We found very good agreement between the strain values measured by our strain sensors and the actual strain values, see figure S8 in the supplementary information. The abovementioned experiments highlight the potential of using CNT–Ecoflex nanocomposite based strain sensors as epidermal devices for human skin motion monitoring.

3.1. Tissue swelling and expansion monitoring

Skin motion detection was performed by using our CNT–Ecoflex nanocomposite based strain sensors. A single strain sensor can detect the strain or mechanical deformation only in one direction defined by the mounting direction of the strain sensor. However, human skin has a complex and multidirectional plane strain field. Since numerous fibers existing underneath skin are tightly grouped and interwoven into bundles, strain fields and their directional components are highly coupled [65]. Therefore, complicated surface skin motion detection is required for several biomedical applications such as wound healing and tissue swelling/expansion monitoring [4, 30]. To characterize the plane skin motion sensing capabilities of our strain sensors, we developed rosette type strain sensors composed of three strain sensors connected in the center with orientation of $120°$ to each other,

as shown in figure 6(a). By using rosette type strain sensors, three components of the strain tensors with respect to the defined coordinate system (i.e. ε_x, ε_y, and γ_{xy}) in a plane deformation can be calculated (see 'Rosette type strain sensors' section in the supplementary information). Figure 6(b) shows the fabricated rosette strain sensor in the original state and when biaxially stretched. To avoid contact noise caused by using rigid electrodes attached to the sensing thin film, we used very high density CNT–Ecoflex nanocomposite thin films as flexible electrodes whose resistance–strain dependency was much smaller than that of a sensing part made of a very low density network. Figure 6(c) illustrates the rosette type strain sensor mounted on the wrist. During bending/relaxing, plane strain is accommodated by the strain sensor. Figure 6(d) shows the normalized resistance changes for sensors a, b, and c under repeated bending/relaxation cycles. The normalized resistance changes of sensor a ($\sim 30\%$) are much higher than those of sensors b and c ($\sim 10\%$). These measurements indicate that larger strain is accommodated by sensor a because of the bending direction. These signals of the individual strain sensors can be potentially used for the calculation of all strain components in the surface deformation. More comprehensive design of multiaxial strain sensor arrays and their application to the strain field analysis of skin will be conducted in future.

4. Conclusions

In this paper, super-stretchable, skin-mountable, and sensitive strain sensors were developed by using CNT percolation network–Ecoflex nanocomposites. The sensitivity of the strain sensors could be controlled though the number density of the CNT percolation network. Excellent hysteresis performance at different strain levels and rates with high linearity and negligible drift are characteristics of the strain sensors. The strain sensors possess super-stretchability with full resistance recovery and high reliability for strains as large as 500%. Skin motion detection was conducted by mounting the strain sensors on different parts of the body as a promising application. The maximum strains accommodated by our strain sensors by the bending of the finger, wrist, and elbow joint were measured to be $\sim$42%, 45% and 63%, respectively. Finally, rosette type strain sensors were developed to detect all strain components in the plane deformation induced by human skin motion. We believe that our developed strain sensors could open up new applications as epidermal electronic devices. They could be used as human motion detectors for virtual reality, robotics, and entertainment applications.

Acknowledgments

References

[1] Amjadi M, Pichitpajongkit A, Lee S, Ryu S and Park I 2014 Highly stretchable and sensitive strain sensor based on silver nanowire-elastomer nanocomposite *ACS Nano* **8** 5154–63

[2] Yan C *et al* 2013 Highly stretchable piezoresistive graphene–nanocellulose nanopaper for strain sensors *Adv. Mater.* **26** 2022–7

[3] Hempel M, Nezich D, Kong J and Hofmann M 2012 A novel class of strain gauges based on layered percolative films of 2D materials *Nano Lett.* **12** 5714–8

[4] Lu N, Lu C, Yang S and Rogers J 2012 Highly sensitive skin-mountable strain gauges based entirely on elastomers *Adv. Funct. Mater.* **22** 4044–50

[5] Yamada T *et al* 2011 A stretchable carbon nanotube strain sensor for human-motion detection *Nat. Nanotechnology* **6** 296–301

[6] Wang Y *et al* 2014 Wearable and highly sensitive graphene strain sensors for human motion monitoring *Adv. Funct. Mater.* **24** 4666–70

[7] Luo S and Liu T 2013 SWCNT/graphite nanoplatelet hybrid thin films for self-temperature-compensated, highly sensitive, and extensible piezoresistive sensors *Adv. Mater.* **25** 5650–7

[8] Takei K *et al* 2010 Nanowire active-matrix circuitry for low-voltage macroscale artificial skin *Nat. Mater.* **9** 821–6

[9] Wang C *et al* 2013 User-interactive electronic skin for instantaneous pressure visualization *Nat. Mater.* **12** 899–904

[10] Webb R C *et al* 2013 Ultrathin conformal devices for precise and continuous thermal characterization of human skin *Nat. Mater.* **12** 938–44

[11] Liu C-X and Choi J-W 2009 An embedded PDMS nanocomposite strain sensor toward biomedical applications, *IEEE Annual Int. Conf. on Engineering in Medicine and Biology Society* pp 6391–4

[12] Giorgino T, Tormene P, Lorussi F, De Rossi D and Quaglini S 2009 Sensor evaluation for wearable strain gauges in neurological rehabilitation *IEEE Trans. Neural Syst. Rehabil. Eng.* **17** 409–15

[13] Lorussi F, Scilingo E P, Tesconi M, Tognetti A and De Rossi D 2005 Strain sensing fabric for hand posture and gesture monitoring *IEEE Trans. Inf. Technol. Biomed.* **9** 372–81

[14] Helmer R, Farrow D, Ball K, Phillips E, Farouil A and Blanchonette I 2011 A pilot evaluation of an electronic textile for lower limb monitoring and interactive biofeedback *Proc. Eng.* **13** 513–8

[15] Liu C-X and Choi J-W 2009 Patterning conductive PDMS nanocomposite in an elastomer using microcontact printing *J. Micromech. Microeng.* **19** 085019

[16] Cohen D J, Mitra D, Peterson K and Maharbiz M M 2012 A highly elastic, capacitive strain gauge based on percolating nanotube networks *Nano Lett.* **12** 1821–5

[17] Rautaray S S and Agrawal A 2011 Interaction with virtual game through hand gesture recognition *Int. Conf. on Multimedia, Signal Processing and Communication Technologies* (*IMPACT*) pp 244–7

[18] Cai L *et al* 2013 Super-stretchable, transparent carbon nanotube-based capacitive strain sensors for human motion detection *Sci. Rep.* **3** 3048

[19] Lipomi D J *et al* 2011 Skin-like pressure and strain sensors based on transparent elastic films of carbon nanotubes *Nat. Nanotechnology* **6** 788–92

[20] Xu F and Zhu Y 2012 Highly conductive and stretchable silver nanowire conductors *Adv. Mater.* **24** 5117–22

[21] Yao S and Zhu Y 2014 Wearable multifunctional sensors using printed stretchable conductors made of silver nanowires *Nanoscale* **6** 2345–52

[22] Mostafalu P and Sonkusale S 2013 Paper-based super-capacitor using micro and nano particle deposition for paper-based diagnostics *IEEE Sensors* pp 1–4

[23] Amjadi M and Park I 2014 Sensitive and stable strain sensors based on the wavy structured electrodes *IEEE 14th Int. Conf. on Nanotechnology* (*Toronto, Canada*) pp 760–3

[24] Fan Q *et al* 2012 The use of a carbon nanotube layer on a polyurethane multifilament substrate for monitoring strains as large as 400% *Carbon* **50** 4085–92

[25] Tadakaluru S, Thongsuwan W and Singjai P 2014 Stretchable and flexible high-strain sensors made using carbon nanotubes and graphite films on natural rubber *Sensors* **14** 868–76

[26] Amjadi M, Pichitpajongkit A, Ryu S and Park I 2014 Piezoresistivity of AG NWS-PDMS nanocomposite *27th Int. Conf. on Micro Electro Mechanical Systems* (*MEMS*) pp 785–8

[27] Xiao X *et al* 2011 High-strain sensors based on ZnO nanowire/polystyrene hybridized flexible films *Adv. Mater.* **23** 5440–4

[28] Zheng M *et al* 2014 Strain sensors based on chromium nanoparticle arrays *Nanoscale* **6** 3930–3

[29] Li X *et al* 2012 Stretchable and highly sensitive graphene-on-polymer strain sensors *Sci. Rep.* **2** 870

[30] Bae S-H, Lee Y, Sharma B K, Lee H-J, Kim J-H and Ahn J-H 2013 'Graphene-based transparent strain sensor *Carbon* **51** 236–42

[31] Tian H *et al* 2013 Scalable fabrication of high-performance and flexible graphene strain sensors *Nanoscale* **6** 699–705

[32] Muth J T *et al* 2014 Embedded 3D printing of strain sensors within highly stretchable elastomers *Adv. Mater.* **26** 6307–12

[33] Xu S, Rezvanian O and Zikry M 2013 Electrothermomechanical modeling and analyses of carbon nanotube polymer composites *J. Eng. Mater. Technol.* **135** 021014

[34] Hu B *et al* 2012 Multi-scale numerical simulations on piezoresistivity of CNT/polymer nanocomposites *Nanoscale Res. Lett.* **7** 1–11

[35] Luo S and Liu T 2013 Structure–property–processing relationships of single-wall carbon nanotube thin film piezoresistive sensors *Carbon* **59** 315–24

[36] Hu N, Fukunaga H, Atobe S, Liu Y and Li J 2011 Piezoresistive strain sensors made from carbon nanotubes based polymer nanocomposites *Sensors* **11** 10691–723

[37] Mirri F *et al* 2012 High-performance carbon nanotube transparent conductive films by scalable dip coating *ACS Nano* **6** 9737–44

[38] Shang Y *et al* 2012 Super-stretchable spring-like carbon nanotube ropes *Adv. Mater.* **24** 2896–900

[39] Chen L *et al* 2011 High-performance, low-voltage, and easy-operable bending actuator based on aligned carbon nanotube/polymer composites *ACS Nano* **5** 1588–93

[40] Shin S R *et al* 2011 Carbon nanotube reinforced hybrid microgels as scaffold materials for cell encapsulation *ACS Nano* **6** 362–72

[41] Ramón-Azcón J *et al* 2013 Dielectrophoretically aligned carbon nanotubes to control electrical and mechanical properties of hydrogels to fabricate contractile muscle myofibers *Adv. Mater.* **25** 4028–34

[42] Singh A V, Mehta K K, Worley K, Dordick J S, Kane R S and Wan L Q 2014 Carbon nanotube-induced loss of multicellular chirality on micropatterned substrate is mediated by oxidative stress *ACS Nano* **8** 2196–205

[43] Parmar K, Mahmoodi M, Park C and Park S S 2013 Effect of CNT alignment on the strain sensing capability of carbon nanotube composites *Smart Mater. Struct.* **22** 075006

[44] Mata A, Fleischman A J and Roy S 2005 Characterization of polydimethylsiloxane (PDMS) properties for biomedical micro/nanosystems *Biomed. Microdevices* **7** 281–93

[45] Qin Q and Zhu Y 2011 Static friction between silicon nanowires and elastomeric substrates *ACS Nano* **5** 7404–10

[46] Lu J, Lu M, Bermak A and Lee Y-K 2007 Study of piezoresistance effect of carbon nanotube-PDMS composite materials for nanosensors *7th IEEE Conf. on Nanotechnology* pp 1240–3

[47] Liang X and Boppart S A 2010 Biomechanical properties of *in vivo* human skin from dynamic optical coherence elastography *IEEE Trans. Biomed. Eng.* **57** 953–9

[48] Pailler-Mattei C, Bec S and Zahouani H 2008 ⟨i⟩ *In vivo* ⟨/i⟩ measurements of the elastic mechanical properties of

human skin by indentation tests *Med. Eng. Phys.* **30** 599–606

[49] Keshoju K and Sun L 2009 Mechanical characterization of magnetic nanowire–polydimethylsiloxane composites *J. Appl. Phys.* **105** 023515

[50] Maxwell R S, Balazs B, Cohenour R and Prevedel E 2003 Aging of silica-filled PDMS/PDPS copolymers in desiccating environments: a DSC and NMR study, *Macromol. Symp.* pp 291–6

[51] Park Y-L, Majidi C, Kramer R, Bérard P and Wood R J 2010 Hyperelastic pressure sensing with a liquid-embedded elastomer *J. Micromech. Microeng.* **20** 125029

[52] Ma P-C, Siddiqui N A, Marom G and Kim J-K 2010 Dispersion and functionalization of carbon nanotubes for polymer-based nanocomposites: a review *Composites Part A* **41** 1345–67

[53] Eom H *et al* 2014 Ag@ Ni core–shell nanowire network for robust transparent electrodes against oxidation and sulfurization *Small* **10** 4171–81

[54] Kim S H, Cho S H, Lee N-E, Kim H M, Nam Y W and Kim Y-H 2005 Adhesion properties of Cu/Cr films on polyimide substrate treated by dielectric barrier discharge plasma *Surf. Coat. Technol.* **193** 101–6

[55] Liu C-X and Choi J-W 2014 Analyzing resistance response of embedded PDMS and carbon nanotubes composite under tensile strain *Microelectronic Eng.* **117** 1–7

[56] Suhr J, Koratkar N, Keblinski P and Ajayan P 2005 Viscoelasticity in carbon nanotube composites *Nat. Mater.* **4** 134–7

[57] Desai A and Haque M 2005 Mechanics of the interface for carbon nanotube–polymer composites *Thin-Walled Struct.* **43** 1787–803

[58] Wong M, Paramsothy M, Xu X, Ren Y, Li S and Liao K 2003 Physical interactions at carbon nanotube-polymer interface *Polymer* **44** 7757–64

[59] Obitayo W and Liu T 2012 A review: carbon nanotube-based piezoresistive strain sensors *J. Sensors* **2012** 652438

[60] Lin L *et al* 2013 Towards tunable sensitivity of electrical property to strain for conductive polymer composites based on thermoplastic elastomer *ACS Appl. Mater. Interfaces* **5** 5815–24

[61] Li C, Thostenson E T and Chou T-W 2007 Dominant role of tunneling resistance in the electrical conductivity of carbon nanotube–based composites *Appl. Phys. Lett.* **91** 223114

[62] Matzeu G, Pucci A, Savi S, Romanelli M and Di Francesco F 2012 A temperature sensor based on a MWCNT/SEBS nanocomposite *Sensors Actuators* A **178** 94–9

[63] Li Y *et al* 2013 Temperature-dependent piezoresistivity in an MWCNT/epoxy nanocomposite temperature sensor with ultrahigh performance *Nanotechnology* **24** 455501

[64] Tjong S, Liang G and Bao S 2007 Electrical behavior of polypropylene/multiwalled carbon nanotube nanocomposites with low percolation threshold *Scr. Mater.* **57** 461–4

[65] Langer K 1978 On the anatomy and physiology of the skin: I. The cleavability of the cutis *Br. J. Plastic Surgery* **31** 3–8